Switching on Fluorescent Emission by Molecular Recognition and Aggregation Dissociation

Naibo Lin, Xiang Yang Liu, Ying Ying Diao, Hongyao Xu,* Chunyan Chen, Xinhua Ouyang, Hongzhi Yang, and Wei Ji*

A generic and effective approach to "switch on" and enhance the two-photon fluorescence (TPF) emission of quenched TPF molecules, i.e., fluorene derivatives, is reported in terms of molecular recognition with a decoupling medium. Such a medium, in this case Bombyx mori silk, can recognize TPF molecules and inhibit the aggregation of the TPF molecules. The designed TPF molecules are 2,7-bis[2-(4-nitrophenyl)ethenyl]-9,9-dibutylfluorene (4NF) and 2,7-bis[2-(4-nitrophenyl)ethenyl]-9,9-dioctylfluorene (8NF), which exhibit suppressed TPF emission owing to molecular-stacking-led aggregation in the solid form. Due to the specific recognition between $-NO_2$ in the quenched fluorescent molecules and –NH groups in silk fibroin molecules, the aggregated molecules of 4NF/8NF molecules are decoupled. This decoupling gives rise to a significant increase in TPF quantum yields. The mechanism is further confirmed by replacing the terminal group $-NO_2$ in 8NF with $-CH_3$ (in 2,7-bis[2-(4-methylphenyl)ethenyl]-9,9-dioctylfluorene; 8MF) to eliminate the possibility of molecular recognition. As predicted, in the case of 8MF the switching-on effect is eliminated. Completely new TPF silk fibers can additionally be applied in real-time 3D high-resolution TPF scaffold bioimaging.

1. Introduction

Efficient two-photon fluorescence (TPF) materials in the solid state are of great scientific and technological relevancy in the areas of 3D fluorescence bioimaging,[1] 3D optical data storage,[2] up-converted lasing,[3] and photodynamic therapy.[4] TPF organic molecules are a special kind of organic molecule that can absorb two photons in the near-IR simultaneously, followed by relaxation in which a single excited photon is emitted in the visible spectrum. Hence, TPF arises from nonlinear two-photon absorption (TPA), while one-photon fluorescence originates from linear one-photon absorption. As reported, the TPF quenching effect, which originates from the aggregation of fluorescence molecules in the solid state, greatly limits the application of potentially excellent fluorescence materials.[5] For two-photon bioimaging, a large two-photon absorption cross section (σ) and a high fluorescence quantum yield (η) are required.[6] In this context, much effort has been devoted to enhancing these two values in solution, especially for TPF organic molecules.[7] The enhancement of the σ value for TPF organic molecules has been quite successful by means of applying particular molecular-design strategies, such as the attachment of electron-rich (π-donor) and/or electron-demanding (π-acceptor) components to the molecules,[8] altering the extent of conjugation path,[9] or increasing coplanarity.[10] However, most TPF materials, such as planar polar molecules, exhibit low η values in solution, and these generally decrease further in the solid state.[11] Therefore, there is an urgent need to identify a novel approach to fabricate TPF materials with enhanced fluorescence efficiency (quantum yield). This efficiency can still be a challenge for TPF materials because of the dramatic concentration quenching of fluorescence in the condensed phase, which arises from intermolecular interactions.

The TPF organic molecules have a rigid and planar structure and a strong tendency to form aggregates by molecular stacking. Such stacking is commonly observed in π-conjugated compounds, and is believed to be the origin of the reduced fluorescence in the solid state.[12] To overcome the problem of fluorescence quenching in the solid form, various approaches have been developed to frustrate the luminophore quenching, which include designing a molecule with a distorted structure,[13] the attachment of steric hindrance groups,[14] and increasing the branches/dimensionality of the molecules.[15] Blending with conventional polymers, for example, has also been used; the fluorescence quantum efficiency of the fluorophore in poly(methyl methacrylate) (PMMA) film is 0.182, while in cyclohexane gel it is 0.108, due to the "rigidochromism" affected by restricted intramolecular twisting motion.[16] Nevertheless, this enhancement is limited, and does not satisfy the high-level requirement for applications such as TPF bioimaging.[17]

Herein, we will tackle this issue based on a new and generic approach to material assembly. The key idea is to identify a

N. B. Lin, Prof. X. Y. Liu, Prof. H. Y. Xu, C. Y. Chen
College of Material Science and Engineering, and State Key Laboratory for Modification of Chemical Fibers and Polymer Materials
Donghua University
Shanghai, 201620, P. R. China
E-mail: phyliuxy@nus.edu.sg; hongyaoxu@163.com
N. B. Lin, Prof. X. Y. Liu, Y. Y. Diao, Dr. X. H. Ouyang, H. Z. Yang, W. Ji
Department of Physics, and Department of Chemistry
National University of Singapore
2 Science Drive 3, Singapore, 117542, Singapore

DOI: 10.1002/adfm.201100649

specific substrate material capable of decoupling the aggregation of fluorescent molecules. This concept includes identifying specific substrate functional groups capable of recognizing and interacting with the TPF molecules, and separating the TPF molecules so that their aggregation is inhibited. This action would not only "switch on" or enhance the fluorescence effect of these fluorescent molecules, but also functionalize the substrate materials with a designated property, i.e., TPF effect, to produce a new class of functional materials. In this regard, we chose three styryl-fluorene derivatives as the quenched fluorescent molecules, and the biocompatible Bombyx mori silk with a special structure as the decoupling medium to dissociate the aggregated TPF styryl-fluorene molecules and thereby meet the stringent requirement of high TPF efficiency. The fluorene derivative is conventional staining agent with low toxicity for living cells, for example, poly(9,9-bis(6-N,N,N-triethylammonium)-hexyl-fluorene phenylene).[18] Symmetrical conjugated styryl-fluorene is a typical TPA molecule with a rigid, planar structure and a strong tendency to form a molecular-stacking arrangement. Bombyx mori silk is an amphiphilic block copolymer and the molecular mass of the dominant high molecular weight protein is ca. 390 KDa.[19] The dominating hydrophobic peptide repeat units self-organize into β-sheet structures, mediated by hydrophobic hydration.[20] Recently, Bombyx mori silk fibers, silk regenerated fibers, films, and sponges have attracted great interest in the fields of biomedicine and high-performance materials,[21] due to their intrinsic functionalities, such as in vitro and in vivo biocompatibility,[19b] robust mechanical properties,[22] and relatively slow biodegradation.[23]

As a key step, we need to identify biomaterials that have the possibility to recognize and interact with the aggregated fluorescent molecules. Specifically, TPF styryl-fluorene molecules should be incorporated into the amorphous region of silk fibers at molecular levels by molecular recognition and interaction. The nitro groups in the fluorene molecules and the amide groups in silk fibroin molecules can be recognized by and interact with each other, which will give rise to decoupling of the aggregated fluorene molecules and, consequently, reactivate and enhance the TPF emission (see **Figure 1**b). Hopefully, the functionalized fluorescent silk fibers will fulfill the demands of various applications, i.e., a silk scaffold with TPF properties for use in noninvasive high-resolution imaging.

2. Results and Discussion

Styryl-fluorene molecules were synthesized with the same terminal nitro groups and different aliphatic chains, namely 2,7-bis[2-(4-nitrophenyl)ethenyl]-9,9-dibutylfluorene (**4NF**) and 2,7-bis[2-(4-nitrophenyl)ethenyl]-9,9-dioctylfluorene (**8NF**). For comparison, 2,7-bis[2-(4-methylphenyl)ethenyl]-9,9-dioctylfluorene (**8MF**) with two methyl terminal groups was also synthesized (cf. Figure 1a). In our method, an amount of the TPF fluorene

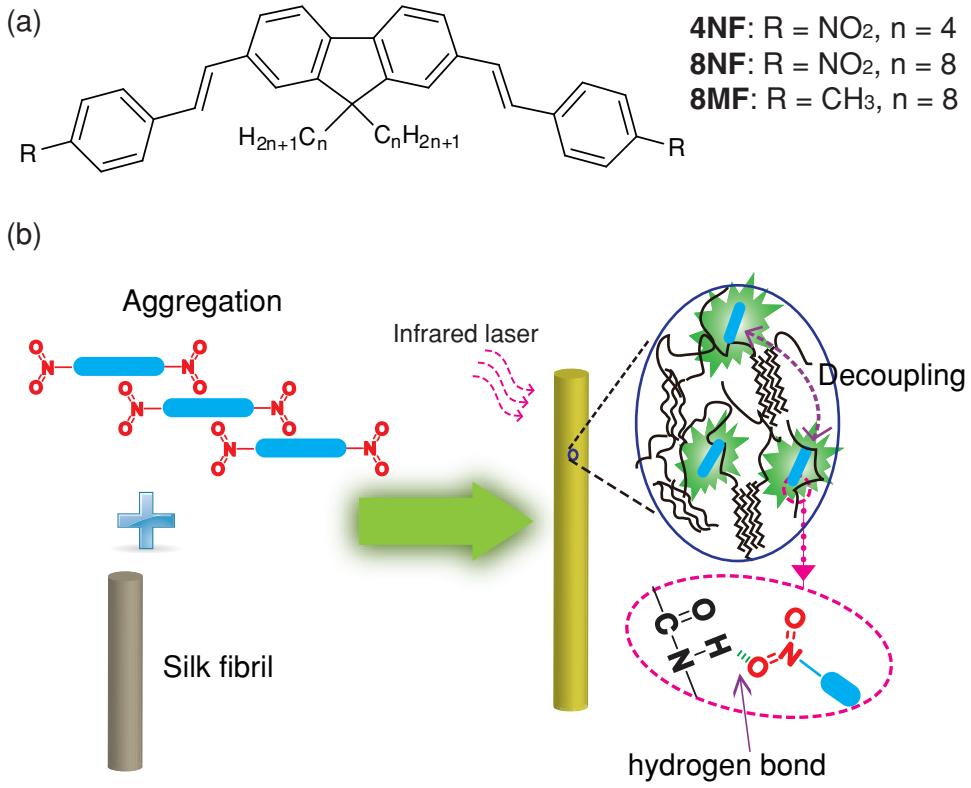

Figure 1. a) Chromophore structures of **4NF**, **8NF**, and **8MF**. b) Proposed model for the silk fibril decoupling effect by the molecular recognition of **4NF**, **8NF**, and **8MF** molecules: the 'silk fibril segments' consist of several β sheets connected by random coils or α helices forming a polypeptide chain network. Two-photon fluorophores **4NF**/**8NF** were decoupled by their specific binding with the amide groups in the silk fibroin molecules,by means of hydrogen bonds.

compound was dissolved in dimethylsulfoxide (DMSO), and sonicated to make a solution. The Bombyx mori silk fibers were immersed in the solution for about 40 minutes at 80 °C. The TPF molecules should adsorb onto the silk fibrils after the evaporation of DMSO at room temperature. The resulting enrichment of TPF molecules will then give rise to cooperative assembly between the TPF molecules and the silk fibroin. The fibers were then rinsed by means of five sonication washes (5 minutes each time) in a soap solution.

2.1. Synthesis and Characteristics

Three different TPF molecules were synthesized by using the Heck reaction (Scheme S1), and their structures characterized. All purified products gave rise to the characteristic spectroscopic data of FTIR, ^{1}H NMR, and elemental analysis corresponding to their expected molecular structures (see Experimental Section for details). UV-Vis absorption and Z-scan measurements were carried out to evaluate one-photon and two-photon absorption properties of all compounds in tetrahydrofuran (THF; Figure S1). The absorption maxima of **4NF** and **8NF** were found to be at 392 and 417 nm, respectively; both red-shifted compared to that of **8MF** (374 nm) because of its electron-withdrawing ability and better electron delocalization caused by the nitro group.[24] The TPA cross-sections for the fluorescent dyes were acquired by open-aperture Z-scan measurements at 780 nm with 450-fs laser pulses at 1-kHz repetition rate. It is striking that the TPA cross-section of 1199 GM for **8NF** is larger than 905 GM for **4NF**, and both are higher than rhodamine 6G, which is about 100 GM.[25] The increase of the TPA cross-section of **8NF** over that of 4NF in THF solution can be attributed to the significant role of longer alkyl chains and the strong polarization effect between the electron-accepting group NO_2 and π-conjugation moieties in the molecular structure.[26] In contrast, the TPA cross-section of **8MF**, in which the electron-withdrawing nitro groups of **8NF** are replaced by methyl groups, is as low as 514 GM.

2.2. One-Photon Fluorescent Emission and Enhancement Caused by Silk Fibroin

Hydrophobic dyes tend to aggregate in two different ways; J aggregates and H aggregates. The absorption band of the J aggregate for some dyes is red-shifted with respect to that of the monomers, while other dyes show a hypsochromic shift for the H aggregate.[27] To validate the structure and energetics of the stacked dimers in the bulk phase, a theoretical calculation was conducted using the Gaussian 09 software suite at the B3LYP/6-31G level of theory. To simplify the calculation, the basic model structure of **8NF** and **8MF** without alkyl chains was selected. It follows that the molecular axes of adjacent **8MF** molecules are parallel to each other, while the molecular planes in the adjacent layers are at an angle. This arrangement suggests that a typical H aggregation occurs of the "herringbone" type (Figure S2a).[28] Molecular modelling reveals that the **8NF** molecules are arranged in a manner similar to that in a J aggregate, where the interacting **8NF** molecules only overlap partially (Figure S2b).

The distribution coefficient *D*, which is the ratio of concentrations of a compound in two immiscible solvents, i.e., chloroform and water, is a measure of the hydrophilicity or hydrophobicity of a chemical substance. The stir-flask method was applied to determine the log *D* of **4NF**, **8NF**, and **8MF**.[29] From Figure S3, it can be seen that log *D* values for **4NF**, **8NF**, and **8MF** are all above 1 within a range of pH = 3.9–8.0, which indicates all three TPF molecules are hydrophobic. This result also rules out the possibility of zwitterionic charge distribution to control intermolecular stacking. Hence, the intermolecular stacking of **4NF**, **8NF**, and **8MF** is caused by aromatic interaction, which is a noncovalent interaction between organic compounds containing aromatic moieties.[30]

The one-photon fluorescence spectra of **4NF**, **8NF** and **8MF** in four organic solvents, *N,N*-dimethylformamide, acetone, tetrahydrofuran, and toluene, are given in Figure S4; the concentration of the solutes was kept at 1.0×10^{-6} M. Our results show that the emission peaks show an increasing red shift as the solvent polarity increases (polarity: *N,N*-dimethylformamide > acetone > tetrahydrofuran > toluene). This shift is caused by the nitro groups in **8NF** and **4NF**, which causes strong dipole–dipole interactions with polar solvent molecules. However, the fluorescence peak of **8MF** shows little difference as the solvent polarity increases. This result indicates that the solvents have little influence on the energy gap between the ground state and the first excited state in the case of linear emission, since the strong polar nitro group in **8NF** is substituted by the nonpolar methyl group in **8MF**. Hence, **8NF** can only interact with solvents by means of weak van der Waals forces, such as induction and dispersion forces.

To check the impact of silk fibroin on the fluorescence emission of the fluorescent molecules after combining with silk fibers, the one-photon fluorescence spectra of the powder of **4NF**, **8NF**, and of their functionalized silks were acquired under the same conditions. It is surprising to see from **Figure 2**a that **4NF** fibers reveal strong fluorescent emission, while the emission from the **4NF** powder is very weak and hardly detectable (the maximal fluorescence spectrum of the **4NF** powder cannot be normalized in Figure 2a). As measured by a calibrated integrating sphere (ISF-513), the quantum yield of **4NF** rises from 1% in the powder form to 22% in the silk fibers. **4NF** molecules in the powder form exhibit a strong molecular stacking/dipole–dipole interaction.[14a,31] The interactions lead to association/aggregation between **4NF** molecules, which enhances the fluorescent emission. In the **4NF** functionalized fibers, the binding of **4NF** molecules to silk fibrils decouples and separates the associated **4NF** molecules. This decoupling eliminates the possibility of the aggregation causing fluorescent emission quenching in the silk fibers, and therefore enhances the fluorescent emission from the functionalized silk fibers. We notice that in the solution state, 4NF aggregates can also dissociate.

The one-photon fluorescent emission enhancement of **8NF** silk fibers is similar to that of **4NF** silk fibers. Due to the side-chain segregation of the alkyl chain, **8NF** in the solid state suffers some quenching. Nevertheless, the overall quenching effect is not as serious as in the case of **4NF**, therefore 8NF still has some fluorescence emission (Figure 2b). Even in this case, the decoupling of **8NF** by the silk fibers still leads to a significant enhancement in fluorescent emission. The quantum value of

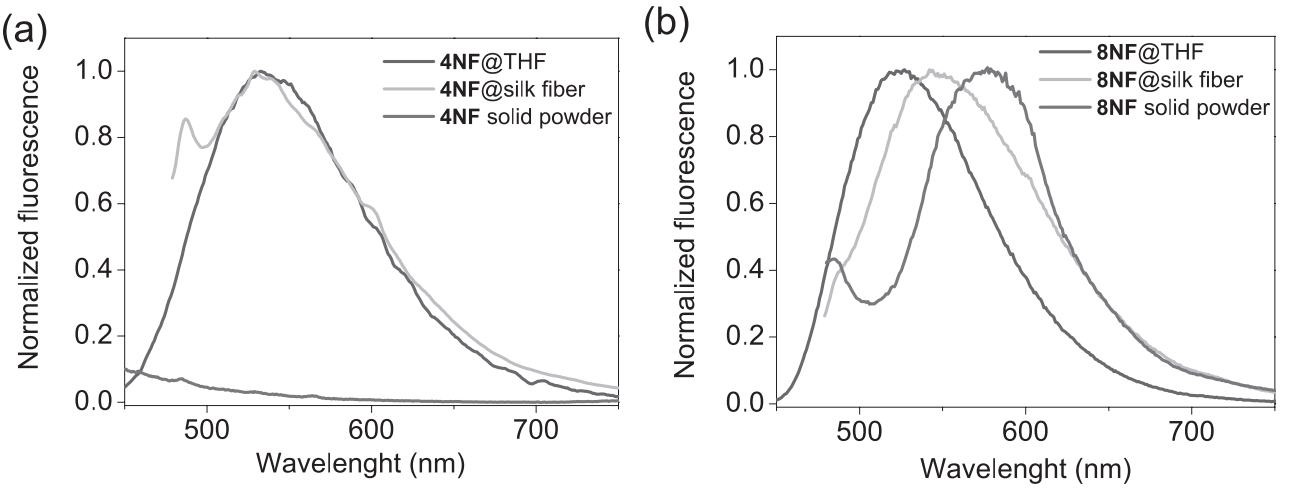

Figure 2. The one-photon fluorescence spectra of a) **4NF** and b) **8NF** in THF solution (concentration = 1.0×10^{-6} M), in silk fibers and in the solid powder form. The excitation wavelengths of the fluorescence spectra were at 392 nm for **4NF**, and 417 nm for **8NF**, which correspond to their maximum absorptions in THF solution. The spectra were normalized at their peak wavelength.

8NF increases from 6% in the powder form to 32% in the silk fibers due to decoupling of aggregation. Moreover, the fluorescence plots of the **8NF** solution, **8NF** fibers, and the powders exhibit a monotonic bathochromic shift in the order of **8NF** solution < **8NF** fibers < **8NF** powder.

2.3. Two-Photon Fluorescence Enhancement

TPF images for obtained fibers were measured by using a two-photon laser scanning confocal microscope (Leica TCS SP2) to study the TPF emission of **4NF**, **8NF**, and **8MF** in silk fibers (wavelength of excitation = 800 nm). **8NF** functionalized silk fibers displayed a very strong TPF. **Figure 3**a–h display precise TPF optical slice images of **8NF** silk fibers. It can be seen that the TPF emission is uniformly distributed from the surface to the centers of the silk fibers. **4NF** silk fibers show similar results. These results indicate that **4NF**/**8NF** molecules strongly interact with the silk fibroin molecules at the molecular level.[32] We also examined the TPF images of **8MF**-functionalized silk fibers. However, the TPF optical slice (Figure S5) shows uneven and very poor TPF emission in contrast that seen in Figure 3a–h. The appearance of the nonuniform and low fluorescence of **8MF** is caused by the weak interaction between **8MF** and silk fibroin by van der Waals forces, in line with the literature.[16]

The TPF spectra of **4NF** and **8NF** silk were studied by femtosecond-pulsed-laser experiments. Figure 3i shows the TPF emission spectra of **4NF** and **8NF** silk fibers. The TPF spectra of **4NF** and **8NF** silk fibers show little difference. The maximum intensities of both **4NF** and **8NF** fibers occur at about 568 nm. Theoretically, fluorescence occurring from a TPF process should exhibit a quadratic dependence on incident intensity; otherwise, the deviation of the dependence will indicate that the trap-state emission could be involved into the TPF process.[33] It can be seen in Figure S6 that all the emission signals of **4NF** and **8NF** silk are proportional to excitation intensity, which confirms the presence of the pure TPF process.

As an important indicator for two-photon emission efficiency, the two-photon action cross-sections ($\sigma\eta$, where σ is the TPA cross-section and η is the value of the fluorescence quantum yield) of **4NF** and **8NF** in the solid form are relatively low: $\sigma\eta_{solid}$ = 905 × 0.01 = 9 GM ($\sigma\eta_{solid}$: the two-photon action cross-section of a molecule in the solid form) and $\sigma\eta_{solid}$ = 1199 × 0.06 = 72 GM, respectively. On the other hand, the $\sigma\eta_{fiber}$ (the two-photon action cross-section of a molecule in silk fibers) of **4NF** and **8NF** silk fibers are enhanced greatly to 905 × 0.22 = 199 GM and 1199 × 0.32 = 384 GM, respectively, which indicates a great enhancement in TPF for both **4NF** and **8NF** silk fibers. Herein, the TPA cross-sections (σ) have been determined by the Z-scan method, and the two-photon fluorescence quantum yield is considered the same as the one-photon fluorescence quantum yield according to the literature.[34] As a result, the **4NF** and **8NF** silk fibers exhibit 22 times and 7 times the two-photon action cross-sections respectively, compared with their counterparts in the solid form.

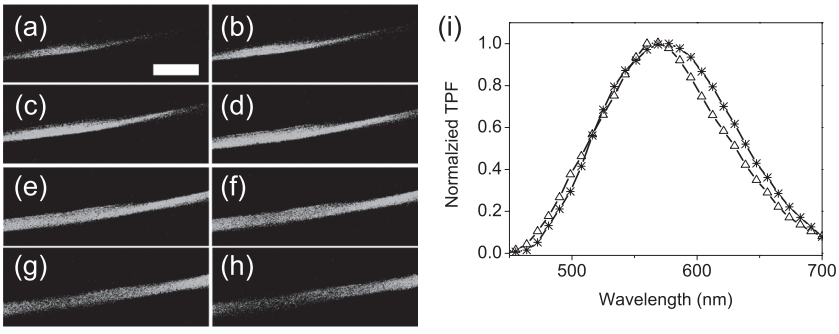

Figure 3. a–h) Consecutive longitudinal section confocal TPF images of **8NF** fiber taken from behind to below the fiber by the serial section scanning method. Scan bar: 73 μm. i) The normalized two-photon fluorescence spectra of **4NF** (symbol: △) and **8NF** (symbol:*) fibers/woven scaffolds.

2.4. Biomolecular "Switch" Based on Molecular Recognition and Decoupling

As suggested by the aforementioned facts and Figure 1b, the attachment of **4NF** and **8NF** in the fluorescent silk fibers is attributed to the molecular recognition and stable interaction between **4NF**/**8NF** and silk fibroin molecules, which prevents the aggregation of **4NF**/**8NF** molecules. To examine this mechanism, we chose **8MF** as an example to investigate. **8MF** is identical to **8NF** except that the terminal group $-NO_2$ in **8NF** is replaced by $-CH_3$ in **8MF**. This change will jeopardize the hydrogen bonding between **8MF** molecules and silk fibroin molecules (via the amide groups). Consequently, even after incorporation into silk fibers, the aggregation among **8MF** molecules won't be inhibited. As mentioned before, Figure S5 reveals that the **8MF** molecules are unevenly distributed in the silk fibers, indicating that they still remain aggregated even though they are incorporated into silk fibers. Meanwhile, the incorporation of **8MF** molecules into silk fibers won't exert much effect on the one-photon fluorescent emission (Figure S7), which can be observed by the following facts: Firstly, the emission spectrum of the **8MF** silk fibers is only slightly shifted from the spectrum of its solid form (peak-to-peak difference is 2 nm), whereas the spectral shift from the **8NF** silk fibers to the **8NF** powder form is about 34 nm. Secondly, the fluorescence efficiency of **8MF** in silk fibers (15%) remains almost unchanged compared with those in the solid form (12%). On the contrary, **8NF** in the silk fibers exhibits bright-yellow emission with an elevated fluorescence efficiency of about 32%, which is significantly higher than that of **8NF** in the solid state (6%). This observation confirms that the TPF emission enhancement is caused by the $-NO_2$ terminal groups of **8NF** molecules, which can interact effectively with the amide groups of the silk fibroins. Obviously, the same reasoning can be applied to **4NF**. The quantum yields ($\eta_{solution}$) of the three TPF molecules in THF were determined by using rhodamine B as standard. For **4NF** and **8NF**, the quantum yields are 0.74 and 0.75, respectively. Although the quantum yields of **4NF**/**8NF** in THF solution are lower than that of **8MF** (0.93), they are dramatically enhanced in the solid state due to molecular recognition and decoupling.

To verify the hydrogen bonding between the nitro group and the amide group, the FTIR spectra of **8NF** powders and **8NF** silk fibers were measured at different temperatures by using a Thermo Nicolet 5700 (see **Figure 4**).[35] Whereas silk fibroin molecules have no absorption in the region of 1300–1360 cm^{-1}, **4NF** and **8NF** have strong characteristic absorption bands in this spectral region, which are attributed to the nitro group vibrations. **8NF** powders at 25 °C show a characteristic nitro vibration band centered at 1340 cm^{-1}, while in the case of **8NF** silk fibers at 25 °C, the nitro absorption maximum of **8NF** shifts toward a lower frequency (a lower wavenumber). This shift is attributed to the change in the chemical environment of the nitro group of **8NF** due to the formation of hydrogen bonds with the amide groups of silk fibroin molecules.[36] Apart from this, hydrogen bonds may be cleaved or weakened by heating the samples (about 100 °C).[37] It follows that after heating to 100 °C, the intensity of the vibrations in the nitro group is weakened and the absorption peak of **8NF** silk fibers shifts back to the high frequency of **8NF** powders, which indicates that the interactions are interrupted as expected.

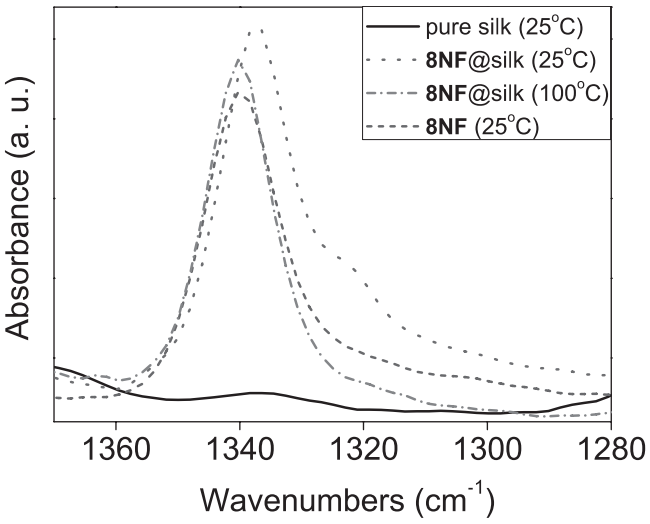

Figure 4. The FTIR spectra of control silk fibers at 25 °C, **8NF** powders at 25 °C, and **8NF** silk fibers at 25 °C and 100 °C.

We notice that as silk fibroins are quite hydrophobic (contact angle≈120°), the hydrogen bonds interactions between **8NF** molecules and silk fibroin molecules can remain very stable once they occur. Similar phenomena are also observed in the infrared spectra of **4NF** silk fibers.

The above results confirm the fact that silk fibroin molecules in silk fibers can "switch on" the fluorescent emission of fluorescent molecules. The mechanism operates via molecular recognition and interaction between nitro groups of the fluorescent molecules and amide groups of the substrate silk materials.

2.5. Silk Scaffold for Bioimaging

Recently, the use of two-photon fluorescence microscopy for biological imaging has received a broad degree of interest because it has several major advantages over current detection technologies, such as its intrinsic optical sectioning capability, little near-IR absorption from endogenous species and water, and large penetration depth.[1c,6,38] In this sense, a functionalized silk scaffold with TPF properties would be valuable for in vitro and in vivo imaging applications. To achieve this goal, the following three key challenges need to be addressed simultaneously: i) the molecules need to have a strong TPA and high TPF efficiency in the silk scaffolds to enable acquisition of high-resolution 3D imaging; ii) the TPF molecules should be distributed uniformly in the silk fibers without jeopardizing the original mechanical properties; iii) the TPF molecules should be almost nontoxic. In all three aspects, our **8NF** silk fibers seem to fulfill these criteria. Some 3D TPF images were taken after a silk scaffold was immersed in RPMI-1640 culture medium in a 24-well tissue culture plate at 37 °C under 5% CO_2. **Figure 5** shows a 3D image of the silk woven scaffold taken one month after seeding in the culture medium. The results show that the scaffolds keep TPF emission well regardless of the immersion time, which further provides the possibility for the scaffolds to be used in imaging with TPF technologies.

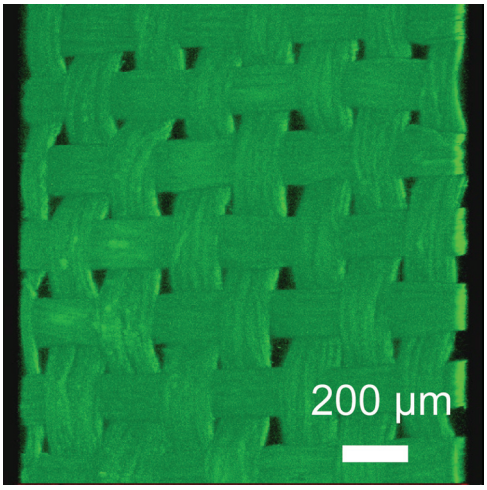

Figure 5. A two-photon fluorescence microscope image showing three-dimensional view of **8NF** woven scaffold in a culture medium.

To check the impact of functionalization on the silk fibers,[39] the mechanical properties of **4NF** and **8NF** silk fibers and pure silk were examined. As indicated by **Figure 6**a and Figure S8, the breaking stress, breaking strain, and breaking energy of the functionalized silk fibers are almost unchanged between the treated and untreated Bombyx mori silk fibers. This result indicates that the treatment of Bombyx mori silk fibers does not deteriorate their mechanical properties. From the electronic scanning microscopic image of the functionalized silk fibers (Figure 6b–d), it can be seen that the diameters and surface morphologies of degummed untreated silks and functionalized silk fibers exhibit no difference, which further verifies that the preparation process does not jeopardize the basic properties of silk fibers.

3. Conclusions

In conclusion, the incorporation of special structure silk fibroin into organic optical materials via hydrogen bonding can effectively overcome the aggregation effect of TPF molecules. The dissociation of **4NF** and **8NF** molecules due to the interactions between the nitro groups of the molecules and amide groups of the silk fibroin substantially enhances their TPF emission. The approach outlined in this manuscript is of general application; for instance, we have confirmed that we can couple other functional molecules or even functionalized quantum dots to silk fibers (work in progress). This result provides a promising route to functionalize silks with intense and homogeneous fluorescence for TPF imaging applications based on the concepts of molecular design and biomolecular recognition.

4. Experimental Section

FTIR spectra were recorded on a Thermo Nicolet 5700 spectrometer. ^{1}H NMR spectra were recorded on a Bruker AVANCE/DMX 400-MHz Bruker NMR spectrometer using chloroform-d ($CDCl_3$). Tetramethylsilane was used as the internal reference for the NMR analyses. UV-Vis spectra were recorded on a Varian Cary 50 spectrometer with a 1-cm^2 quartz cell. Fluorescence spectra were recorded on a FP-6600 (Jasco Inc.) spectrophotometer using a quartz cell with an optical path length of 1 mm. The quantum yield of the solid silk fibers and the powder were determined on the spectrophotometer with an integrating sphere (ISF-513). Scanning electron microscopy images were recorded on a JEOL JSM-6700F field electron microscope operating at 5 kV. An Instron MicroTester was used to measure the force–extension characteristics of the silk. A thread was fixed between two hooks of the instrument, which had a gauge length of 20 mm and a measured error of 0.1 mm. The thread was stretched until it broke and the strain rate was 50% per minute. The experiments were operated at 22 °C and humidity was kept at 65%.

Z-Scan Measurements: TPA cross-section values for both dyes were determined by means of open-aperture Z-scan measurements at 780 nm with 450-fs laser pulses at 1-kHz repetition rate. The laser beam was generated by a mode-locked Ti: sapphire laser, which was seeded by a Ti: sapphire regenerative amplifier. The laser pulses with near-Gaussian spatial and temporal profiles were focused onto 1-mm-thick quartz cuvette using a lens of focal length of 15 cm. Moreover, the Z-scan experimental system was calibrated using a piece of cadmium sulfide bulk crystal because this sample possesses large TPA at the wavelength of 780 nm and was well-investigated in our laboratory. In theory, the normalized transmittance for the open aperture can be written as Equation 1:

$$T(z, s = 1) = \sum_{m=0}^{\infty} \frac{[-q_0(z)]^m}{(m+1)^{3/2}}, \text{ for } |q_0| < 1 \quad (1)$$

where $q_0(z) = \beta I_0 L_{eff}/(1+z^2/z_0^2)$ where β is the TPA coefficient, I_0 is the intensity of laser beam at focus ($z = 0$), $L_{eff} = [1-\exp(-\alpha_0 L)]/\alpha_0$ is the effective

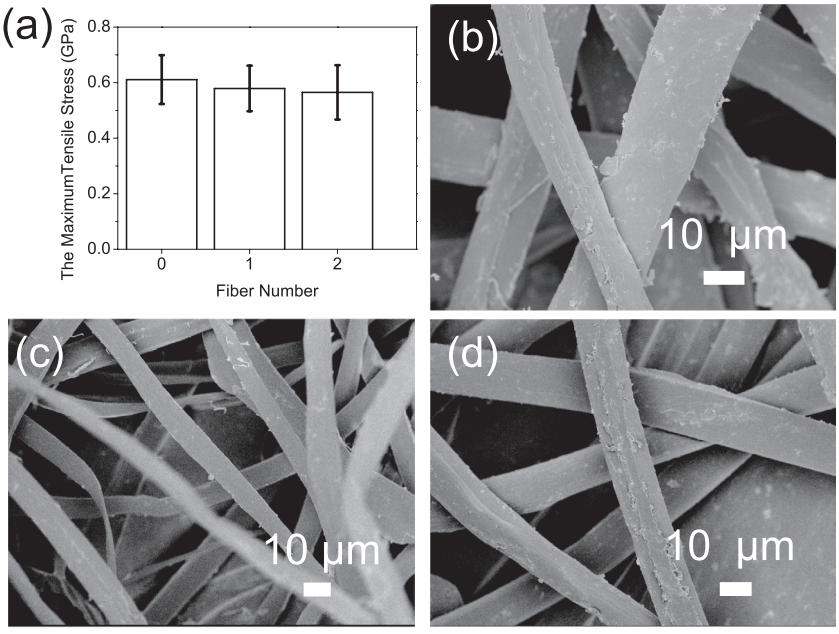

Figure 6. a) The breaking stress of pure Bombyx mori silk (0), **4NF** fibers (1) and **8NF** fibers (2), respectively. b) Scanning electron microscopy of **8NF** functionalized silk fibers, c) **4NF** fiber, and d) control silk fibers.

thickness, α_0 is the linear absorption coefficient, L is the sample thickness, z_0 is the diffraction length of the laser beam, and z is the sample position.[40] The TPA cross-section σ is calculated by using Equation 2:

$$\sigma = h\nu\beta / N \quad (2)$$

where N is the number of molecules per cm^3 and $h\nu$ is the excitation photon energy. The TPA cross-section σ is expressed in Göppert Mayer (GM) units, in which 1 GM = 1×10^{-50} cm^4 s $photon^{-1}$ $molecule^{-1}$.

Two-Photon Fluorescence Measurement: TPF imaging and spectrum of fibers were performed using Leica TCS SP2 laser scanning confocal microscope with a Ti:sapphire laser (Mira Optima 900F, Coherent) as the excitation source. The laser is tuned at 780 nm with 0.5 mW power after the objective and provides ca. 100-fs pulses at a repetition rate of 76 MHz. The details of the two-photon technique experimental setup are described elsewhere.[41]

*2,7-Dibromo-9,9-dibutylfluorene (**1**)*: 1-Bromobutane (3.97 g, 29.0 mmol) was added by syringe to a mixture of 2,7-dibromofluorene (3.88 g, 12.0 mmol), tetrabutyl ammonium bromide (0.0225 g, 0.0975 mmol), and 3.75 mL of 50% aqueous NaOH in DMSO (50.0 mL). The reaction mixture was stirred at room temperature for 3 h. The mixture was poured into H_2O (500 mL), and was then extracted three times with dichloromethane. The combined organic layers were dried over anhydrous $MgSO_4$ and decolorized using active carbon. The solvent was removed under reduced pressure. The crude product was purified by recrystallization in hexane to yield a colorless crystal (90%). M.p. 112 °C; ^{1}H NMR (400 MHz, $CDCl_3$, δ): 7.56 (d, 2H, Ar H), 7.49 (m, 4H, Ar H), 1.96 (m, 4H, CH_2), 1.14 (m, 4H, CH_2), 0.74 (t, 6H, CH_3), 0.62 (m, 4H, CH_2); IR (KBr): ν = 2950, 2868 (m; CH), 1599, 1515, 858 (w; Ar).

*2,7-Dibromo-9,9-dioctylfluorene (**2**)*: This was prepared as above from 1-bromooctane and 2,7-dibromofluorene. Yield 83%. M.p. 43 °C; ^{1}H NMR (400 MHz, $CDCl_3$, δ): 7.51 (d, 2H, Ar H), 7.45 (m, 4H, Ar H), 1.90 (m, 4H, CH_2), 1.30–1.00 (m, 36H, CH_2), 0.87 (t, 6H, CH_3), 0.59 (m, 4H, CH_2); IR (KBr): ν = 2972, 2879 (m; CH), 1595, 1517, 861 (w; Ar).

p-Nitrostyrene: Triphenylphosphine (26.23 g, 100 mmol) and *p*-nitrobenzyl bromide (21.60 g, 100 mmol) were added in anhydrous methanol (100 mL). The mixture was stirred and refluxed at 70 °C for 3 h. After evaporating the solvent, the resulting powder was dissolved into 150 mL formaldehyde aqueous solution (concentration 37%), 20 mL NaOH aqueous solution was then added dropwise with stirring for 4 h at 0 °C. The precipitate was filtered and washed with water and dichloromethane. The product was then purified by column chromatography (SiO_2, toluene/n-hexane, 1:1) to yield 10.50 g (84.7%) yellow liquid. ^{1}H NMR (400 MHz, $CDCl_3$, δ): 8.18 (d, 2H, Ar H), 7.53 (d, 2H, Ar H), 6.78 (m, 1H, CH), 5.93 (d, 1H, CH_2), 5.50 (d, 1H, CH_2).

*2,7-Bis[2-(4-nitrophenyl)ethenyl]-9,9-dibutylfluorene (**4NF**)*: 2,7-Dibromo-9,9-dibutylfluorene (1.09 g, 2.5 mmol), $Pd(OAc)_2$ (5.6 mg, 2.5×10^{-2} mmol), triphenylphosphine (26.25 mg, 0.1 mmol), *p*-nitrostyrene (5.75 mmol), and Et_3N (5 mL) were combined in a screw-cap vial and heated to 100 °C for 48 h. The reaction mixture was cooled to room temperature and distilled. The mixture was extracted with CH_2Cl_2, dried over $MgSO_4$, and concentrated. The crude product was purified by column chromatography with petroleum ether/EtOAc (50:1). The crude product was recrystallized from n-hexane to give a solid in 68% yield. M.p. 204 °C; ^{1}H NMR (400 MHz, $CDCl_3$, δ): 8.25 (d, 4H, Ar H), 7.70 (m, 6H, Ar H), 7.55 (t, 2H, Ar H), 7.38 (d, 2H, CH), 7.23 (d, 2H, CH), 2.02 (s, 4H, CH_2), 1.13 (m, 4H, CH_2), 0.81 (t, 6H, CH_3), 0.68 (s, 4H, CH_2); IR (KBr): ν = 2924, 2852 (m; CH), 1630, 1514, 865 (m; Ar), 1379 (s; NO_2). Calcd for $C_{37}H_{36}N_2O_4$: C 77.60, H 6.33, N 4.89; found: C 77.57, H 6.36, N 4.88.

*2,7-Bis[2-(4-nitrophenyl)ethenyl]-9,9-dioctylfluorene (**8NF**)*: This was prepared as above for **4NF**. Yield: 60%, M.p. 127 °C, ^{1}H NMR (400 MHz, $CDCl_3$, δ): 8.26 (d, 4H, Ar H), 7.73 (m, 6H, Ar H), 7.58 (t, 2H, Ar H), 7.39 (d, 2H, Ar H), 7.23 (d, 2H, Ar H), 2.06 (s, 4H, CH_2), 1.15 (m, 20H, CH_2), 0.81 (t, 6H, CH_3), 0.68 (s, 4H, CH_2). IR (KBr): ν = 2950, 2923 (m; CH), 1592, 1515, 819 (w, Ar), 1340 (s, NO_2). Calcd for $C_{45}H_{28}N_4O_7$: C 79.15, H 7.38, N 4.10; found: C 79.27, H 7.40, N 4.13.

*2,7-Bis[2-(4-methylphenyl)ethenyl]- 9, 9-dioctylfluorene (**8MF**)*: This was prepared as above for **4MF**, in 50% yield. M.p. 121 °C, ^{1}H NMR (400 MHz, $CDCl_3$, δ): 7.67 (d, 2H, Ar H), 7.47 (m, 4H, Ar H), 7.19 (t, 4H, Ar H), 2.39 (s, 6H, CH_3), 2.03 (t, 4H, CH_2), 1.08–1.29 (m, 20H, CH_2), 0.83 (t, 6H, CH_3), 0.69 (s, 4H, CH_2); IR (KBr): ν = 2927, 2852 (m; CH), 1604, 1464, 819 (m; Ar). Calcd for $C_{47}H_{56}$: C 90.90, H 9.09; found: C 90.97, H 9.05.

Two-Photon Fluorescence Fibers and Woven Scaffold Preparation: Silk woven scaffolds (2 × 2 cm) were fabricated from degummed silk fibers. Silk fibers/woven scaffolds were obtained from Bombxy mori silkworm silk (Liangguang 2). Raw silk fibers/scaffolds were degummed in an aqueous solution containing 5g·L^{-1} sodium carbonate, 10 g·L^{-1} soap at 85 °C for 45 minutes, then rinsed using DI water. The fibers/scaffolds were dried at room temperature for two days. In a typical process, degummed silk fibers/scaffolds were immersed in a reaction bath with a dimethylsulfoxide (DMSO) solution (0.15 mL) consisting of 4% **4NF** (on the weight of fibers [o.w.f.]). The silk sample sealed in test tubes were carried out at 80 °C for about 40 minutes. Then, the silk fibers/scaffolds were removed and dried at room temperature. The functionalized silk fibers were rinsed with distilled water, and sonicated for 5 minutes. The same rinsing procedure was repeated five times.

Supporting Information

Supporting Information is available from the Wiley Online Library or from the author.

Acknowledgements

This work is financially supported by AcRF Tier 1 (R-144-000-264-112), NUS FOS Seed Funding (N-144-000-045-001), the National Natural Science Fund of China (Grant Nos. 20974018, 20971021, 51073031 and 21171034), National Oversea Scholar Cooperation Research Fund of China (No. 50928301), and the China MOE Chang Jiang Scholars Program.

Received: March 24, 2011
Revised: September 12, 2011
Published online: November 18, 2011

[1] a) W. Denk, J. H. Strickler, W. W. Webb, *Science* **1990**, *248*, 73; b) D. R. Larson, W. R. Zipfel, R. M. Williams, S. W. Clark, M. P. Bruchez, F. W. Wise, W. W. Webb, *Science* **2003**, *300*, 1434; c) M. Pawlicki, H. A. Collins, R. G. Denning, H. L. Anderson, *Angew. Chem. Int. Ed.* **2009**, *48*, 3244; d) J. Jiang, H. W. Gu, H. L. Shao, E. Devlin, G. C. Papaefthymiou, J. Y. Ying, *Adv. Mater.* **2008**, *20*, 4403; e) P. Tayalia, C. R. Mendonca, T. Baldacchini, D. J. Mooney, E. Mazur, *Adv. Mater.* **2008**, *20*, 4494.

[2] a) J. H. Strickler, W. W. Webb, *Adv. Mater.* **1993**, *5*, 479; b) C. C. Corredor, Z. L. Huang, K. D. Belfield, A. R. Morales, M. V. Bondar, *Chem. Mater.* **2007**, *19*, 5165; c) C. C. Corredor, Z. L. Huang, K. D. Belfield, *Adv. Mater.* **2006**, *18*, 2910.

[3] a) J. J. Jasieniak, I. Fortunati, S. Gardin, R. Signorini, R. Bozio, A. Martucci, P. Mulvaney, *Adv. Mater.* **2008**, *20*, 69; b) F. He, L. L. Tian, X. Y. Tian, H. Xu, Y. H. Wang, W. J. Xie, M. Hanif, J. L. Xia, F. Z. Shen, B. Yang, F. Li, Y. G. Ma, Y. Q. Yang, J. C. Shen, *Adv. Funct. Mater.* **2007**, *17*, 1551; c) G. Jordan, T. Kobayashi, W. J. Blau, S. Pfeiffer, H. H. Horhold, *Adv. Funct. Mater.* **2003**, *13*, 751; d) S. L. Oliveira, D. S. Correa, L. Misoguti, C. J. L. Constantino, R. F. Aroca, S. C. Zilio, C. R. Mendonca, *Adv. Mater.* **2005**, *17*, 1890.

[4] a) W. R. Dichtel, J. M. Serin, C. Edder, J. M. J. Frechet, M. Matuszewski, L. S. Tan, T. Y. Ohulchanskyy, P. N. Prasad, *J. Am. Chem. Soc.* **2004**, *126*, 5380; b) J. Arnbjerg, A. Jimenez-Banzo, M. J. Paterson, S. Nonell, J. I. Borrell, O. Christiansen, P. R. Ogilby, *J. Am. Chem. Soc.* **2007**, *129*, 5188; c) D. Gao, R. R. Agayan, H. Xu, M. A. Philbert, R. Kopelman, *Nano Lett.* **2006**, *6*, 2383; d) M. Velusamy, J. Y. Shen, J. T. Lin, Y. C. Lin, C. C. Hsieh, C. H. Lai, C. W. Lai, M. L. Ho, Y. C. Chen, P. T. Chou, J. K. Hsiao, *Adv. Funct. Mater.* **2009**, *19*, 2388; e) Z. D. Qi, D. W. Li, P. Jiang, F. L. Jiang, Y. S. Li, Y. Liu, W. K. Wong, K. W. Cheah, *J. Mater. Chem.* **2011**, *21*, 2455.

[5] a) S. Kim, Q. Zheng, G. S. He, D. J. Bharali, H. E. Pudavar, A. Baev, P. N. Prasad, *Adv. Funct. Mater.* **2006**, *16*, 2317; b) S. Y. Hsueh, C. C. Lai, Y. H. Liu, Y. Wang, S. M. Peng, S. H. Chiu, *Org. Lett.* **2007**, *9*, 4523; c) J. J. Gassensmith, J. M. Baumes, B. D. Smith, *Chem. Commun.* **2009**, 6329; d) J. Q. Qu, J. Y. Zhang, A. C. Grimsdale, K. Mullen, F. Jaiser, X. H. Yang, D. Neher, *Macromolecules* **2004**, *37*, 8297; e) Z. S. Wang, N. Koumura, Y. Cui, M. Takahashi, H. Sekiguchi, A. Mori, T. Kubo, A. Furube, K. Hara, *Chem. Mater.* **2008**, *20*, 3993.
[6] G. S. He, L. S. Tan, Q. Zheng, P. N. Prasad, *Chem. Rev.* **2008**, *108*, 1245.
[7] a) S. J. Chung, S. J. Zheng, T. Odani, L. Beverina, J. Fu, L. A. Padilha, A. Biesso, J. M. Hales, X. W. Zhan, K. Schmidt, A. J. Ye, E. Zojer, S. Barlow, D. J. Hagan, E. W. Van Stryland, Y. P. Yi, Z. G. Shuai, G. A. Pagani, J. L. Bredas, J. W. Perry, S. R. Marder, *J. Am. Chem. Soc.* **2006**, *128*, 14444; b) J. H. Liu, Y. L. Mao, M. J. Huang, Y. Z. Gu, W. F. Zhang, *J. Phys. Chem. A.* **2007**, *111*, 9013.
[8] a) S. J. Chung, M. Rumi, V. Alain, S. Barlow, J. W. Perry, S. R. Marder, *J. Am. Chem. Soc.* **2005**, *127*, 10844; b) S. Mori, K. S. Kim, Z. S. Yoon, S. B. Noh, D. Kim, A. Osuka, *J. Am. Chem. Soc.* **2007**, *129*, 11344.
[9] a) L. Beverina, J. Fu, A. Leclercq, E. Zojer, P. Pacher, S. Barlow, E. W. Van Stryland, D. J. Hagan, J. L. Bredas, S. R. Marder, *J. Am. Chem. Soc.* **2005**, *127*, 7282; b) M. Williams-Harry, A. Bhaskar, G. Ramakrishna, T. Goodson, M. Imamura, A. Mawatari, K. Nakao, H. Enozawa, T. Nishinaga, M. Iyoda, *J. Am. Chem. Soc.* **2008**, *130*, 3252; c) Q. D. Zheng, G. S. He, P. N. Prasad, *Chem. Mater.* **2005**, *17*, 6004; d) A. J. Qin, J. W. Y. Lam, H. C. Dong, W. X. Lu, C. K. W. Jim, Y. Q. Dong, M. Haussler, H. H. Y. Sung, I. D. Williams, G. K. L. Wong, B. Z. Tang, *Macromolecules* **2007**, *40*, 4879.
[10] a) T. K. Ahn, K. S. Kim, D. Y. Kim, S. B. Noh, N. Aratani, C. Ikeda, A. Osuka, D. Kim, *J. Am. Chem. Soc.* **2006**, *128*, 1700; b) S. K. Pati, T. J. Marks, M. A. Ratner, *J. Am. Chem. Soc.* **2001**, *123*, 7287.
[11] a) T. R. Krishna, M. Parent, M. H. V. Werts, L. Moreaux, S. Gmouh, S. Charpak, A. M. Caminade, J. P. Majoral, M. Blanchard Desce, *Angew. Chem. Int. Ed.* **2006**, *45*, 4645; b) K. Ogawa, H. Hasegawa, Y. Inaba, Y. Kobuke, H. Inouye, Y. Kanemitsu, E. Kohno, T. Hirano, S. Ogura, I. Okura, *J. Med. Chem.* **2006**, *49*, 2276.
[12] a) H. B. Fu, D. B. Xiao, J. N. Yao, G. Q. Yang, *Angew. Chem. Int. Ed.* **2003**, *42*, 2883; b) S. Sreejith, K. P. Divya, A. Ajayaghosh, *Chem. Commun.* **2008**, 2903; c) Z. Q. Xie, B. Yang, G. Cheng, L. L. Liu, F. He, F. Z. Shen, Y. G. Ma, S. Y. Liu, *Chem. Mater.* **2005**, *17*, 1287; d) S. Ozcelik, D. L. Akins, *J. Phys. Chem. B.* **1999**, *103*, 8926; e) R. Deans, J. Kim, M. R. Machacek, T. M. Swager, *J. Am. Chem. Soc.* **2000**, *122*, 8565; f) M. Levitus, K. Schmieder, H. Ricks, K. D. Shimizu, U. H. F. Bunz, M. A. Garcia-Garibay, *J. Am. Chem. Soc.* **2001**, *123*, 4259.
[13] S. W. Thomas, G. D. Joly, T. M. Swager, *Chem. Rev.* **2007**, *107*, 1339.
[14] a) H. Y. Woo, B. Liu, B. Kohler, D. Korystov, A. Mikhailovsky, G. C. Bazan, *J. Am. Chem. Soc.* **2005**, *127*, 14721; b) W. Z. Yuan, P. Lu, S. M. Chen, J. W. Y. Lam, Z. M. Wang, Y. Liu, H. S. Kwok, Y. G. Ma, B. Z. Tang, *Adv. Mater.* **2010**, *22*, 2159.
[15] a) H. Y. Woo, D. Korystov, A. Mikhailovsky, T. Q. Nguyen, G. C. Bazan, *J. Am. Chem. Soc.* **2005**, *127*, 13794; b) J. S. Yang, J. L. Yan, *Chem. Commun.* **2008**, 1501; c) H. Zhang, Z. C. Cui, Y. Wang, K. Zhang, X. L. Ji, C. L. Lu, B. Yang, M. Y. Gao, *Adv. Mater.* **2003**, *15*, 777; d) J. N. Moorthy, P. Natarajan, P. Venkatakrishnan, D. F. Huang, T. J. Chow, *Org. Lett.* **2007**, *9*, 5215.
[16] S. Y. Park, M. K. Nayak, B. H. Kim, J. E. Kwon, S. Park, J. Seo, J. W. Chung, *Chem. Eur. J.* **2010**, *16*, 7437.
[17] a) T. Y. Yu, C. K. Ober, S. M. Kuebler, W. H. Zhou, S. R. Marder, J. W. Perry, *Adv. Mater.* **2003**, *15*, 517; b) S. Putthanarat, R. K. Eby, R. R. Naik, S. B. Juhl, M. A. Walker, E. Peterman, S. Ristich, J. Magoshi, T. Tanaka, M. O. Stone, B. L. Farmer, C. Brewer, D. Ott, *Polymer* **2004**, *45*, 8451.
[18] a) K. Y. Pu, K. Li, B. Liu, *Adv. Mater.* **2010**, *22*, 643; b) K. Y. Pu, K. Li, X. H. Zhang, B. Liu, *Adv. Mater.* **2010**, *22*, 4186; c) N. Tian, Q. H. Xu, *Adv. Mater.* **2007**, *19*, 1988.
[19] a) S. Ghosh, S. T. Parker, X. Wang, D. L. Kaplan, J. A. Lewis, *Adv. Funct. Mater.* **2008**, *18*, 1883; b) C. Vepari, D. L. Kaplan, *Prog. Polym. Sci.* **2007**, *32*, 991; c) Z. Z. Shao, F. Vollrath, *Nature.* **2002**, *418*, 741; d) J. H. Shi, S. X. Lua, N. Du, X. Y. Liu, J. X. Song, *Biomaterials* **2008**, *29*, 2820.
[20] a) F. V. David Porter, *Adv. Mater.* **2009**, *21*, 487; b) N. Du, X. Y. Liu, J. Narayanan, L. A. Li, M. L. M. Lim, D. Q. Li, *Biophys. J.* **2006**, *91*, 4528; c) N. Du, Z. Yang, X. Y. Liu, Y. Li, H. Y. Xu, *Adv. Funct. Mater.* **2011**, *21*, 772.
[21] a) A. M. Collins, N. J. V. Skaer, T. Cheysens, D. Knight, C. Bertram, H. I. Roach, R. O. C. Oreffo, S. Von-Aulock, T. Baris, J. Skinner, S. Mann, *Adv. Mater.* **2009**, *21*, 75; b) F. G. Omenetto, D. L. KapLan, *Nat. Photon.* **2008**, *2*, 641; c) D. H. Kim, J. Viventi, J. J. Amsden, J. L. Xiao, L. Vigeland, Y. S. Kim, J. A. Blanco, B. Panilaitis, E. S. Frechette, D. Contreras, D. L. Kaplan, F. G. Omenetto, Y. G. Huang, K. C. Hwang, M. R. Zakin, B. Litt, J. A. Rogers, *Nat. Methods* **2010**, *9*, 511.
[22] C. Jiang, X. Wang, R. Gunawidjaja, Y. H. Lin, M. K. Gupta, D. L. Kaplan, R. R. Naik, V. V. Tsukruk, *Adv. Funct. Mater.* **2007**, *17*, 2229.
[23] a) A. Vasconcelos, G. Freddi, A. Cavaco-Paulo, *Biomacromolecules* **2008**, *9*, 1299; b) A. T. Quitain, H. Daimon, K. Fujie, S. Katoh, T. Moriyoshi, *Ind. Eng. Chem. Res.* **2006**, *45*, 4471.
[24] a) K. L. Chan, M. Sims, S. I. Pascu, M. Ariu, A. B. Holmes, D. D. C. Bradley, *Adv. Funct. Mater.* **2009**, *19*, 2147; b) X. Y. Su, S. Y. Guang, H. Y. Xu, X. Y. Liu, S. Li, X. Wang, Y. Deng, P. Wang, *Macromolecules* **2009**, *42*, 8969; c) X. Y. Su, H. Y. Xu, Q. Z. Guo, G. Shi, J. Y. Yang, Y. L. Song, X. Y. Liu, *J. Polym. Sci., Part A: Polym. Chem.* **2008**, *46*, 4529.
[25] M. A. Albota, C. Xu, W. W. Webb, *Appl. Opt.* **1998**, *37*, 7352.
[26] S. Yao, K. D. Belfield, *J. Org. Chem.* **2005**, *70*, 5126.
[27] a) E. E. Jelley, *Nature* **1936**, *138*, 1009; b) G. Scheibe, *Angew. Chem.* **1937**, *50*, 212; c) A. Eisfeld, J. S. Briggs, *Chem. Phys.* **2006**, *324*, 376.
[28] A. J. Cadby, J. Partee, J. Shinar, S. J. Martin, C. W. Spangler, D. D. C. Bradley, P. A. Lane, *Phys. Rev. B* **2002**, *65*, 245202.
[29] D. N. Brooke, A. J. Dobbs, N. Williams, *Ecotox. Environ. Safe.* **1986**, *11*, 251.
[30] A. Sygula, F. R. Fronczek, R. Sygula, P. W. Rabideau, M. M. Olmstead, *J. Am. Chem. Soc.* **2007**, *129*, 3842.
[31] G. P. Bartholomew, M. Rumi, S. J. K. Pond, J. W. Perry, S. Tretiak, G. C. Bazan, *J. Am. Chem. Soc.* **2004**, *126*, 11529.
[32] Q. Q. Dang, S. D. Lu, S. Yu, P. C. Sun, Z. Yuan, *Biomacromolecules* **2010**, *11*, 1796.
[33] J. He, G. D. Scholes, Y. L. Qu, W. Ji, *J. Appl. Phys.* **2008**, *104*, 1.
[34] Y. Tian, C. Y. Chen, Y. J. Cheng, A. C. Young, N. M. Tucker, A. K. Y. Jen, *Adv. Funct. Mater.* **2007**, *17*, 1691.
[35] a) S. C. Yin, H. Y. Xu, W. F. Shi, Y. C. Gao, Y. L. Song, B. Z. Tang, *Dyes Pigments* **2006**, *71*, 138; b) L. C. Cesteros, J. R. Isasi, I. Katime, *Macromolecules* **1993**, *26*, 7256.
[36] V. Granzhan, S. Semenenko, P. Zaitsev, *J. Appl. Spectrosc.* **1968**, *9*, 929.
[37] J. R. Isasi, L. C. Cesteros, I. Katime, *Macromolecules* **1994**, *27*, 2200.
[38] a) Y. Yang, A. Dubois, X. P. Qin, J. Li, A. El Haj, R. K. Wang, *Phys. Med. Biol.* **2006**, *51*, 1649; b) Y. Sun, H. Y. Tan, S. J. Lin, H. S. Lee, T. Y. Lin, S. H. Jee, T. H. Young, W. Lo, W. L. Chen, C. Y. Dong, *Microsc. Res. Techniq.* **2008**, *71*, 140.
[39] A. M. Collins, N. J. V. Skaer, T. Gheysens, D. Knight, C. Bertram, H. I. Roach, R. O. C. Oreffo, S. Von Aulock, T. Baris, J. Skinner, S. Mann, *Adv. Mater.* **2009**, *21*, 75.
[40] X. H. Ouyang, H. P. Zeng, W. Ji, *J. Phys. Chem. B* **2009**, *113*, 14565.
[41] F. G. Haj, P. J. Verveer, A. Squire, B. G. Neel, P. I. H. Bastiaens, *Science* **2002**, *295*, 1708.